IOP Publishing | Astro Ltd
Laser Physics Letters
Laser Phys. Lett. **11** (2014) 125107 (6pp)
doi:10.1088/1612-2011/11/12/125107

2.05 μm ytterbium–holmium doped all-fiber gain-switched pulsed laser pumped at 1064 nm

A V Kir'yanov, Yu O Barmenkov and V P Minkovich

Centro de Investigaciones en Optica, Loma del Bosque 115, Col. Lomas del Campestre, Leon 37150, Guanajuato, Mexico

E-mail: kiryanov@cio.mx

Received 27 September 2014
Accepted for publication 14 October 2014
Published 6 November 2014

Abstract

The novel, extremely simple to assemble, design of a ~2.05 μm ytterbium–holmium co-doped all-fiber laser (YHDFL) oscillating in the gain-switching pulsed regime is reported. The YHDFL is pumped by a 1064 nm ytterbium doped fiber laser, while pulsing at ~2.05 μm, is accomplished using an acousto-optic modulator placed between the two lasers. At the optimal conditions, the YHDFL produces a train of very stable, single per modulation period, pulses, 1 μJ in energy and 1 μs in duration at a 3 dB level, at repetition rates of 50…60 kHz.

Keywords: fiber laser, ytterbium, holmium, gain-switching

(Some figures may appear in colour only in the online journal)

1. Introduction

Pulsed fiber lasers (FLs) operating in the 2 μm range are important sources for numerous applications including remote sensing, material processing, micromachining, medicine, optical parametric oscillators, etc. Usually pulsed regimes in such lasers are implemented using active and passive Q-switching [1–3] or passive mode-locking [4].

Gain switching (GS) is the other technique that permits the generation of high-contrast single pulses (or their 'per-demand' engineered trains), sequencing at high repetition rates (tens…hundreds kHz) and scaled from a few nanoseconds to ~1 μs, through 'straightforward' pulsed pumping, or (as is the case of the present work) through an external pump-light modulation biased to a laser, for instance, to a FL. Due to their simplicity in experimental realization, FLs at GS have demonstrated a certain success in the recent years. The GS technique has been applied to a wide class of FLs based on Nd^{3+}, Tm^{3+}, Er^{3+}, Yb^{3+} and Ho^{3+} doped fibers [5–16]. The use of Bragg gratings (FBGs) as cavity couplers of a GS-FL allows it to be assembled in 'all-fiber' geometry, which enables a characteristic spectral bandwidth of pulsing limited by ~100 pm [12, 17]. The chirp-free GS-FL's operation makes it suitable for a number of applications, e.g. Doppler lidars [12], nonlinear frequency conversion [17], etc. The basic principle of GS realized in the current work, i.e. external pump modulation, relies on a properly organized switching pump power on and off. Once the pump is switched on, the active dopant's laser level is populated to a degree, sufficient for enrolling in the cavity the relaxation oscillation process of photon generation, which happens at the initial stage of the transience to continuous-wave (CW) operation; as a consequence, the first, the second and further laser 'pulses' (in fact, spikes of relaxation oscillations) arise. To segregate the first spike of relaxation oscillations, one needs to switch the pump off at a certain moment depending on the repetition frequency, as the corresponding analysis shows. This scenario of control over the pump modulation permits the realization of a 'sole-pulse-per-modulation-cycle' GS, most relevant for practice requirements.

In this letter, we report the first,to the best to our knowledge, application of the GS technique to an ytterbium–holmium co-doped FL (YHDFL), targeted at the 'pulse per demand' operation. The laser was assembled in the simplest Fabry–Perot cavity geometry, employing a piece of Yb^{3+}–Ho^{3+} co-doped fiber (YHDF) and a pair of standard FBG-couplers, reflecting at ~2.05 μm. The YHDFL was pumped by a commercial ytterbium-doped FL (YDFL) at a 'standard' wavelength,

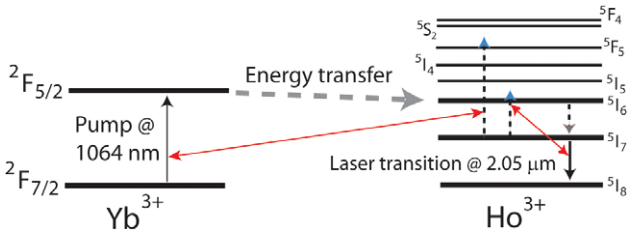

Figure 1. YHDF: energy levels of the Yb^{3+} and Ho^{3+} ions. The processes involved at ~2.05 μm lasing under 1.064 μm pumping are shown by arrows (dotted arrows starting from the Ho^{3+} laser level ($^5I_7$) schematize the possible ESA transitions at the pump and laser wavelengths, which are nonetheless negligible at pumping at 1064 nm).

1064 nm; an 'uncommon' pump wavelength's choice–out of both the co-dopants (Yb^{3+} and Ho^{3+}) resonant absorption peaks – has been nonetheless demonstrated to be relevant for effective ~2.05 μm CW lasing [18]. The pump light was modulated by means of a commercial fibered acousto-optic modulator (AOM), optimized for the pump wavelength, when biasing a rectangular control signal permits switching the AOM to the 'open' (highly transmitting) state with the rise time of ~20 ns. That is, the YHDFL was arranged in an all-fiber design, adequate for practical needs. The route of accomplishing and the featuring details of the YHDFL's GS pulsing, through varying the AOM's open state duration ('window,' or 'gate') and repetition (modulation) frequency, are discussed in the following.

2. Basic properties of YHDF

The YHDF is a competitive candidate for ~2 μm lasing [18]. In this fiber, the Ho^{3+} ion is indirectly pumped to state $^5I_6$ via the energy transfer process from the Yb^{3+} ion's upper level ($^2F_{5/2}$) (see figure 1), populated by the pump light at 1064 nm, i.e. aside from the ground-state absorption (GSA) peak of Yb^{3+} (~976 nm). Fast non-radiative relaxation $^5I_6 \rightarrow {}^5I_7$ in the Ho^{3+} subsystem provides its inversion, sufficient for lasing at ~2 μm.

Interest in YHDFs [19–21] stems from the extraordinary features of the Yb^{3+} subsystem: The Yb^{3+} ion is unique among other rare-earth ions in the sense that it has the highest absorption and emission cross-sections and that it is free from excited-state absorption (ESA), given by its two-level energy scheme. Furthermore, Yb^{3+} can be embedded into silica glass up to very high concentrations. Regarding the Ho^{3+} subsystem in YHDF, let us emphasize the absence of ESA from the $^5I_7$ (Ho^{3+}) laser level, at both the pump (1064 nm) and laser (~2.05 μm) wavelengths: Refer again to figure 1, where it is seen that possible ESA transitions, shown as dotted arrows, mismatch the energy gaps between the energy levels of the Ho^{3+} ions.

The home-made YHDF is fabricated from a preform obtained through the modified chemical vapor deposition (MCVD) process in tandem with the solution doping (SD) technique; the final fiber is drawn using a standard fiber-draw tower facility. The outer clad and doped core diameters of the YHDF are 124.5 μm and 5.7 μm, respectively and the cutoff wavelength and numerical aperture (NA)–0.97 μm and 0.13. Thus, the fabricated YHDF supports single-mode propagation at both the laser and pump wavelengths. The doping levels of Yb_2O_3 and Ho_2O_3 are measured (at the preform stage) to be ~6.0 wt.% and ~0.6 wt.%, respectively. Furthermore, Al_2O_3 (~2.0 wt.%) and GeO_2 (~0.5 wt.%) are embedded into the core glass for engineering Δn and also (Al_2O_3) for diminishing the ions' clustering. The other YHDF's parameters are specified in [18].

3. Experimental setup

The experimental setup of the GS-YHDFL is shown in figure 2. A 5 m piece of YHDF is pumped using a commercial YDFL with fiber output (IPG-Polus: Model PYL-10 LP) through a standard AOM (A-A Opto-Electronic), optimized for 1064 nm. The AOM's insertion loss is ~3 dB and the maximum optical power supported is 5 W. The AOM operates at a driving frequency of 110 MHz; the GS regime is obtained by applying a rectangular signal from a pulse generator (Stanford Research Systems: model DG645) to the AOM's driver. The YHDF cavity is formed by two FBGs, both centered at ~2.0475 μm, with reflection coefficients of 91% (FBG 1, a 'rear' reflector) and 72% (FBG 2, an output reflector), respectively. A long-pass filter (Thorlabs: Model FEL1100, not shown) is placed at the YHDFL's output in spectrally-selective measurements, which provides a rejection of the pump light (at 1.064 μm) at a >21 dB level while transmitting ~2.05 μm light (at the YHDFL's operation wavelength) at a ~60% level.

The YHDFL output signal is measured by an InGaAs photo-detector (PD), sensitive to ~2 μm radiation (Thorlabs: Model DET10D, rise-time 25 ns), or by a Silicon PD (New Focus, model: 2031), not sensitive in a 2 μm range, connected to an oscilloscope (Tektronix: Model TDS 3032), or by a power–meter (Thorlabs: Model S314-C). During the experiments, we varied both the AOM's gate and repetition rate, whereas the pump power at the AOM's output was kept constant (2.5 W). The GS-YHDFL was not optimized in the sense of the cavity's Q-factor: The reflectivity of the rear coupler (FBG1) was a long way from 100% and that of the output coupler (FBG2) was not low enough as would be necessary; furthermore, we noticed inevitable losses on the splices between the fibers forming the cavity, which had different waveguide parameters. On the other hand, the YHDFL's operation was optimized in the sense of the right choice of the YHDF length, as demonstrated in [18], the best efficiency of the CW operation of an YHDFL based on the same active fiber is accomplished by using a YHDF length measuring 5…6 m, which provides <10% of the pump remnant at the output (viz, >90% pump power absorbed in the YHDF).

4. Experimental results and discussion

The YHDFL was easily turned to a pulsed operation by applying the GS technique, i.e. through modulating the pump light by biasing a rectangular control signal to the AOM's driver (see figure 2). By means of switching the AOM's transmission

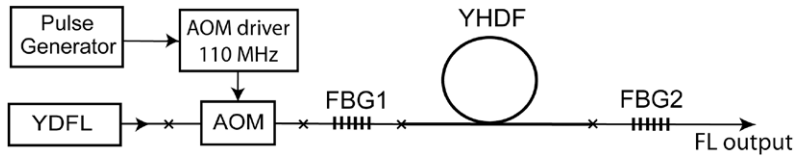

Figure 2. Experimental setup of the GS-YHDFL (the crosses indicate fiber splices).

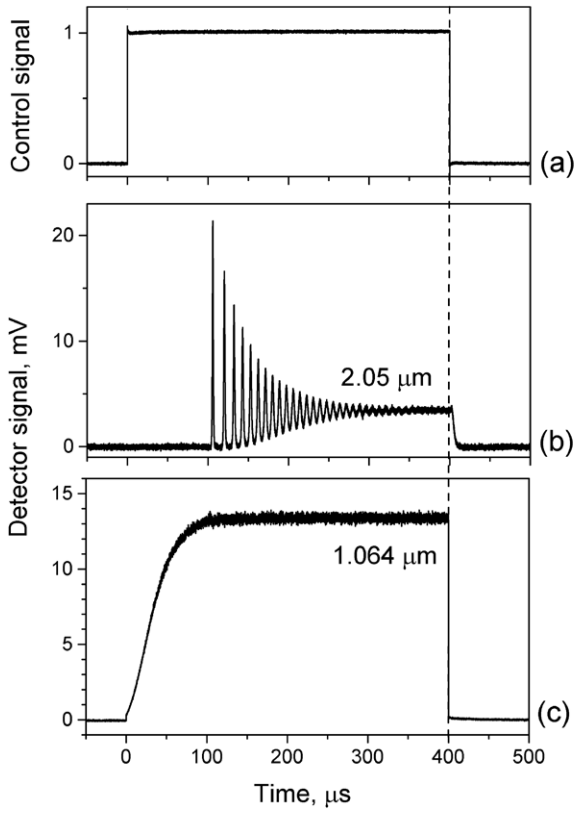

Figure 3. The normalized control signal biased to the AOM's driver (*a*); the relaxation oscillations of the YHDFL measured by the InGaAs PD with the long-pass filter rejecting pump wavelength (*b*); (*c*) the pump power remnants measured by Silicon PD. Zero-time corresponds to the moment when the AOM is switched on.

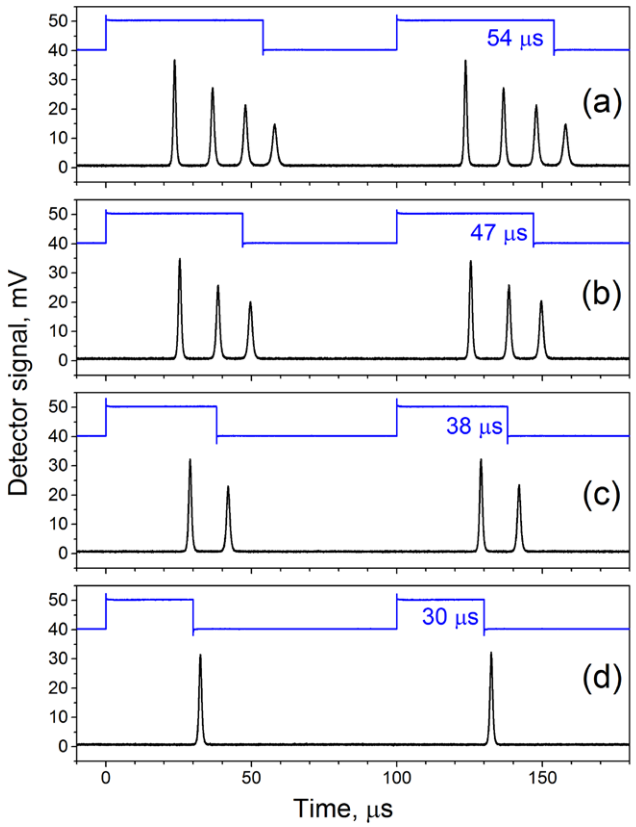

Figure 4. Oscilloscope traces of the YHDFL's relaxation oscillations, captured at f_{AOM} = 10 kHz and various AOM's gates. In each picture the upper curve is a control signal biased to the AOM's driver and the bottom one is the oscilloscope trace registered; the AOM's gate is marked near the control signal.

on and off–at different repetition rates (f_{AOM}) (in the domain measured by units to a hundred kHz) and at controllable durations of the AOM's gate–a variety of pulsing regimes at ~2.05 μm were obtained.

Firstly, to reveal what happens in general with the YHDFL at GS, we studied the generation of the spikes of the relaxation oscillation (see figure 3), followed by a transient to CW, at a low repetition rate (1 kHz) and the chosen long AOM's gate (400 μs).

It is seen that when the AOM is switched on, the laser oscillates in a 'classic' regime of relaxation oscillations with a number of spikes arising at the beginning of the process (see figure 3(*b*), where the laser signal was measured using the long-pass filter rejecting the pump wavelength). The first (biggest) spike is delayed by approximately 100 μs with respect to the moment of the AOM switching on; its width at a 3 dB level is ~1.5 μs. The characteristic laser relaxation frequency, measured at the moment of the relaxation oscillations' fading (at t >300 μs), is ~110 kHz. Figure 3(*c*) demonstrates the 'bleaching' of the YHDF at the pump wavelength. The detailed analysis of the pattern shows that the fiber's transmission increases by ~17 dB during the first 100 μs after switching the AOM on, provided the YHDF has been fully 'discharged' after a preceding modulation cycle (note that 2.05 μm lasing decays in ~5 μs after switching the AOM off, see figure 3(*b*), at t >400 μs).

Next we studied the transformations of the relaxation oscillations at ~2.05 μm while varying the AOM's gate, but keeping f_{AOM} fixed (at 10 kHz). Some representative oscilloscope traces, demonstrating the lasing transformations' features, are shown in figure 4.

From this figure, we can see that the number of spikes of the relaxation process decreases with reducing the AOM's gate (compare snapshots (*a*)–(*d*)). At the same time, the first spike delays the moment of the AOM's opening for a longer time with reducing the gate, which is explained by a decrease

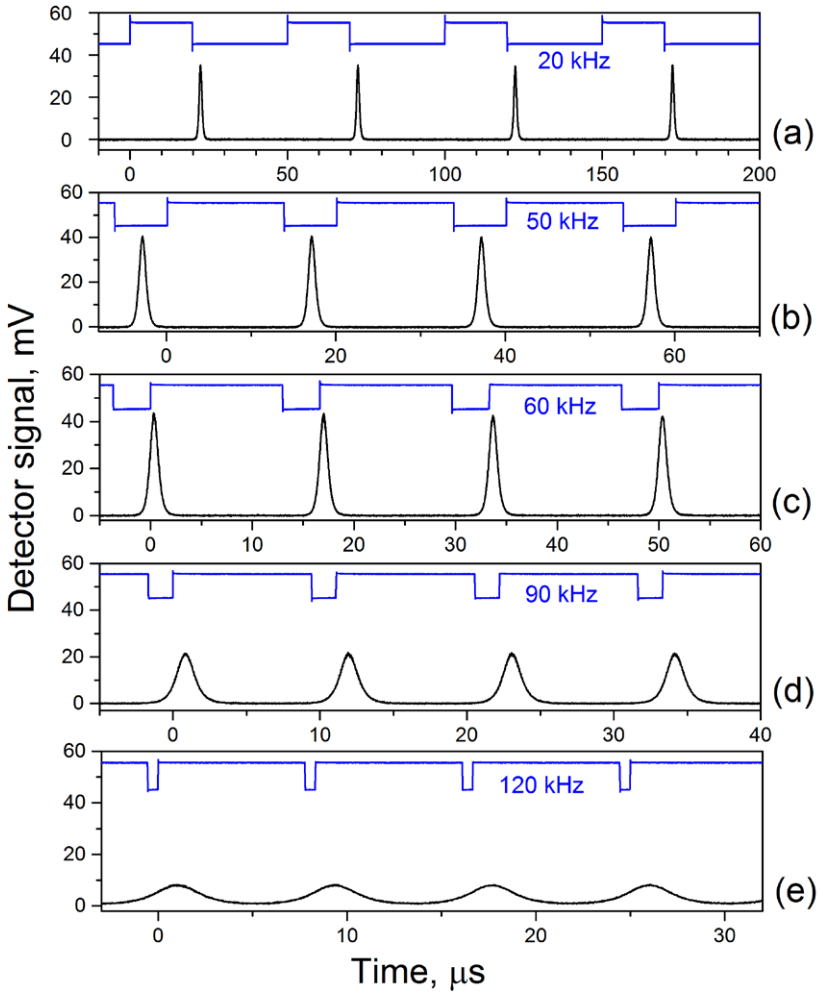

Figure 5. Examples of the optimized GS pulses obtained at different AOM's repetition rates. In each picture the upper curve is a control signal biased to the AOM's driver (in r.u.) and the bottom one is the oscilloscope trace of GS pulses; the AOM's gate is marked near the control signal.

in the pump average power launched to the YHDF due to a reduction in the AOM's on/off ratio. A stable 'sole-pulse-per-gate' operation of the laser is registered for the AOM's gate equal to ≈30 μs (see figure 4(*d*)); the width of a single pulse (which is in fact the first spike of the relaxation oscillations) measured at a 3 dB level is 1.1 μs. In other words, a 30 μs AOM's gate is optimal for single-pulse 'infinite' generation at a repetition rate of 10 kHz (note that the AOM's on/off ratio in this case is ≈0.43).

A similar optimization routine is applied for a wider range of AOM's gates, which leads us to reveal an overall optimization of GS pulsing, in the sense of determining the maximal pulse power and minimal pulse duration, allowed by the current YHDFL's version. A few essential examples of this optimized GS operation of the laser are given in figure 5.

As we can see in this figure, in all circumstances s single-pulse (per modulation cycle) oscillation is accomplished, and the higher the AOM's repetition rate, the higher the AOM's on/off ratio: For instance, at f_{AOM} = 20, 60 and 90 kHz this ratio is 0.67, 3.5 and 5.7, respectively. Furthermore, at lower repetition rates ($f_{AOM} \leq 40$ kHz) the optimized 'GS-pulses'

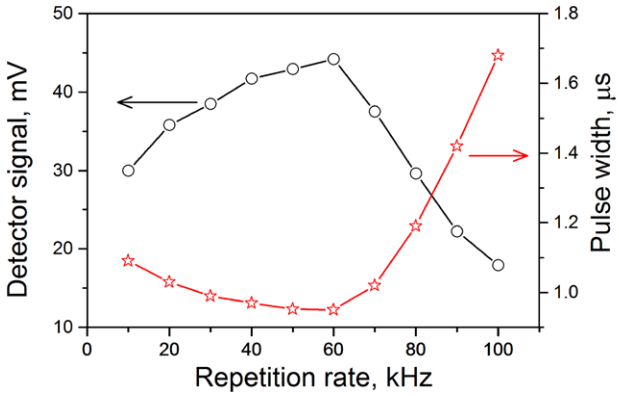

Figure 6. The GS pulse amplitude (circles, left scale) and width (stars, right scale) as functions of the AOM's repetition rate.

reach the maximal power just after switching the AOM off (see figures 4(*d*) and 5(*a*)), whereas at higher repetition rates ($f_{AOM} \geq 60$ kHz) the pulses' peaks are observed just after switching the AOM on (for the next cycle of the active fiber's 'charging'). The latter happens because the relative time interval (normalized to the repetition period) necessitated for

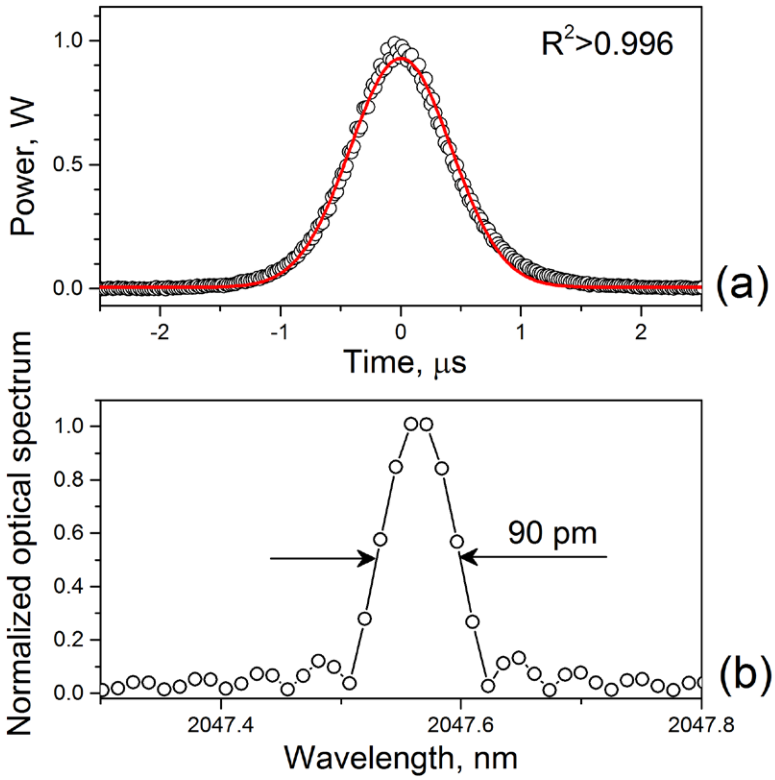

Figure 7. (*a*) The GS pulse detected at f_{AOM} = 60 kHz (circles: experimental points; red solid line: Gaussian fit). (*b*) Normalized optical spectrum of GS pulsing, measured at f_{AOM} =60 kHz (circles: experimental points).

establishing an optimal GS-pulse increases with increasing f_{AOM}. An example of the intermediate situation, occurring between the featured sub-regimes, is shown in figure 5(*b*), for f_{AOM} = 50 kHz, where a GS-pulse arises in the middle of the AOM's closed state. Finally, at very high repetition rates (f_{AOM} > 100 kHz) the GS pulsing transforms into a quasi-sinusoidal oscillation (see figure 5(*e*)), resembling the so-called period-1 regime of a FL's dynamics at the sinusoidal pump modulation (see for example [22, 23]).

Another detail of the GS operation deserving attention is the law that the dependences of the amplitude and width of the optimal GS-pulses versus the repetition rate obey, as shown in figure 6. It is seen that the best result–when the pulse amplitude reaches a maximum and simultaneously, the pulse width becomes minimal–is obtained at f_{AOM} ≈60 kHz (as compared with figure 5(*c*)). On the left of this f_{AOM}-value, both these parameters change modestly (and so, in fact, the optimal operation is fulfilled within the f_{AOM}-range being 50…60 kHz), whereas on the right they are transformed to a much greater degree (where the transition from GS pulsing to sinusoidal-like oscillations happens). The maximal GS-pulse power and energy (both observed at the optimal conditions: f_{AOM} ≈60 kHz; AOM's on/off ratio ≈3.5) were measured to be ~1 W and ~1 μJ, respectively.

The GS-pulses, obtained at the repetition rates less than 100 kHz were found to be fitted well by the Gaussian function. An example of a GS-pulse fitted by this function is shown in figure 7(*a*), for f_{AOM} = 60 kHz (the residual sum of fitting is better than 0.996). The optical spectrum of GS pulsing, which corresponds to the optimal conditions, is shown in figure 7(*b*); we employed an optical spectrum analyzer at these measurements (Thorlabs: Model 203), turned to a resolution of 37 pm in a 2 μm range. Therefore, one can reveal that the spectral width of GS lasing is ≈90 pm at a 3 dB level, which is only slightly (by ~25%) bigger than the line-width at a CW operation in a similar laser: As compared with the results reported in [18] .

5. Conclusion

We demonstrate an YHDF-based all-fiber pulsed laser oscillating in the GS regime (being a kind of external pump-light modulation) at ~2.05 μm, employing a 1.064 μm YDFL as a pump source. GS pulsing is accomplished by means of the use of a standard fibered AOM, placed in between the YDFL and YHDFL, which produces a rectangular modulation of the pump power (2.5 W in the AOM's open state). The YHDFL is assembled in a simple Fabry–Perot geometry, with two FBGs centered at 2047.5 nm, being used as cavity couplers, thus constituting an all-fiber configuration of the device. It is shown that both the pulse amplitude and pulse duration strongly depend on the AOM's repetition rate. A proper choice of the AOM's gate, for each value of the repetition rate, permits the turning of the laser to the regime, in which a sole Gaussian pulse per AOM's gate is produced. At the optimal conditions, as found in the current experimental arrangement (the AOM's repetition rate being 60 kHz and the AOM on/off ratio being 3.5), the YHDFL produces a train of stable GS-pulses with a peak power of ~1 W, energy of ~1 μJ and a

duration of less than 1 μs. The YDFLS's optical spectrum at GS pulsing is ~90 pm, measured at a 3 dB level. At very high repetition rates (in excess of 100 kHz), the laser transits to the regime of quasi-sinusoidal oscillations. The high-contrast and long-term stability of the produced ~2.05 μm GS pulses ought to be emphasized, being inherent to the YHDFL feature, as attractive for applications.

Acknowledgments

The authors acknowledge the partial support from the CONACyT, Mexico through the Project No. 167945.

References

[1] Jung M and Lee J H 2013 Actively Q-switched, thulium–holmium-codoped fiber laser incorporating a silicon-based, variable-optical-attenuator-based Q switch *Appl. Opt.* **52** 2706
[2] Chamorovskiy A Y, Marakulin A V, Kurkov A S, Leinonen T and Okhotnikov O G 2012 High-repetition-rate Q-switched holmium fiber laser *IEEE Photon. J.* **4** 679
[3] Sholokhov E M, Marakulin A V, Kurkov A S and Tsvetkov V B 2011 All-fiber Q-switched holmium laser *Laser Phys. Lett.* **8** 382
[4] Chamorovskiy A, Marakulin A V, Ranta S, Tavast M, Rautiainen J, Leinonen T, Kurkov A S and Okhotnikov O G 2012 Femtosecond mode-locked holmium fiber laser pumped by semiconductor disk laser *Opt. Lett.* **37** 1448
[5] Zenteno L A, Snitzer E, Po H, Tumminelli R and Hakimi F 1989 Gain switching of a Nd^{3+}-doped fiber laser *Opt. Lett.* **14** 671
[6] Jackson S D and King T A 1998 Efficient gain-switched operation of a Tm-doped silica fiber laser *IEEE J. Quantum Electron.* **34** 779
[7] Nakagami H, Araki S and Sakata H 2011 Gain-switching pulse generation of Tm-doped fiber ring laser pumped with 1.6 μm laser diodes *Laser Phys. Lett.* **8** 301
[8] Yang J, Tang Y and Xu J 2013 Hybrid-pumped, linear-polarized, gain-switching operation of a Tm-doped fiber laser *Laser Phys. Lett.* **10** 055104
[9] Tsai T Y, Ma H H, Fang Y C, Tsao H X and Lin S T 2011 Self-balanced Q- and gain-switched erbium all-fiber laser *AIP Adv.* **1** 032155
[10] Jackson S D, Dickinson B C and King T A 2002 Sequence lasing in a gain-switched Yb^{3+}, Er^{3+}-doped silica double-clad fiber laser *Appl. Opt.* **41** 1698
[11] Wu K S, Ottaway D, Munch J, Lancaster D G, Bennetts S and Jackson S D 2009 Gain-switched holmium-doped fibre laser *Opt. Express* **17** 20872
[12] Geng J, Wang Q, Luo T, Case B, Jiang S, Amzajerdian F and Yu J 2012 Single-frequency gain-switched Ho-doped fiber laser *Opt. Lett.* **37** 3795
[13] Yang W Q, Zhang B, Hou J, Xiao R, Song R, and Liu Z J 2013 Gain-switched and mode-locked Tm/Ho-codoped 2 μm fiber laser for mid-IR supercontinuum generation in a Tm-doped fiber amplifier *Laser Phys. Lett.* **10** 045106
[14] Tang Y L, Li F and Xu J Q 2013 Narrow-pulse-width gain-switched thulium fiber laser *Laser Phys. Lett.* **10** 035101
[15] Yang J, Tang Y and Xu J 2013 Development and applications of gain-switched fiber lasers [Invited] *Photon. Res.* **1** 52
[16] Swiderski J, Maciejewska M, Kwiatkowski J and Mamajek M 2013 An all-fiber, resonantly pumped, gain-switched, 2 μm Tm-doped silica fiber laser *Laser Phys. Lett.* **10** 015107
[17] Larsen C, Giesberts M, Nyga S, Fitzau O, Jungbluth B, Hoffmann H D and Bang O 2013 Gain-switched all-fiber laser with narrow bandwidth *Opt. Express* **21** 12302
[18] Kir'yanov A V, Minkovich V P and Barmenkov Y O 2014 All-fiber 2.05 μm continuous-wave ytterbium–holmium laser pumped at 1.064 μm *IEEE Photon. Technol. Lett.* **26** 1924
[19] Jackson S D and Mossman S 2003 Diode-cladding-pumped Yb^{3+}, Ho^{3+}-doped silica fiber laser operating at 2.1 μm *Appl. Opt.* **42** 3546
[20] Kir'yanov A V, Minkovich V P, Barmenkov Y O, Gamez M A M and Martinez-Rios A 2005 Multi-wavelength visible up-converted luminescence in novel heavily doped ytterbium–holmium silica fiber under low-power IR diode pumping *J. Lumin.* **111** 1
[21] Kir'yanov A V, Barmenkov Y O, Minkovich V P and Andres M V 2007 Nonlinear transmission coefficient of ytterbium–holmium fiber at the wavelength 978 nm *Laser Phys.* **17** 71
[22] Pisarchik A N, Barmenkov Y O and Kir'yanov A V 2003 Experimental characterization of the bifurcation structure in an erbium-doped fiber laser with pump modulation *IEEE J. Quantum Electron.* **39** 1567
[23] Pisarchik A N, Kir'yanov A V and Barmenkov Y O 2005 Dynamics of an erbium-doped fiber laser with pump modulation: theory and experiment *J. Opt. Soc. Am.* B **22** 2107